

# Hysteresis in $\eta/s$ for QFTs dual to spherical black holes

---

**Mariano Cadoni, Edgardo Franzin and Matteo Tuveri**

*Dipartimento di Fisica, Università di Cagliari & INFN, Sezione di Cagliari  
Cittadella Universitaria, 09042 Monserrato, Italy*

*E-mail:* [mariano.cadoni@ca.infn.it](mailto:mariano.cadoni@ca.infn.it), [edgardo.franzin@ca.infn.it](mailto:edgardo.franzin@ca.infn.it),  
[matteo.tuveri@ca.infn.it](mailto:matteo.tuveri@ca.infn.it)

**ABSTRACT:** We define and compute the (analogue) shear viscosity to entropy density ratio  $\tilde{\eta}/s$  for the QFTs dual to spherical AdS black holes both in Einstein and Gauss-Bonnet gravity in five spacetime dimensions. Although in this case, owing to the lack of translational symmetry of the background,  $\tilde{\eta}$  has not the usual hydrodynamic meaning, it can be still interpreted as the rate of entropy production due to a strain. At large and small temperatures, we find that  $\tilde{\eta}/s$  is a monotonic increasing function of the temperature. In particular, at large temperatures it approaches a constant value, whereas, at small temperatures, when the black hole has a regular, stable extremal limit,  $\tilde{\eta}/s$  goes to zero with scaling law behaviour. Whenever the phase diagram of the black hole has a Van der Waals-like behaviour, i.e. it is characterised by the presence of two stable states (small and large black holes) connected by a meta-stable region (intermediate black holes), the system evolution must occur through the meta-stable region and temperature-dependent hysteresis of  $\tilde{\eta}/s$  is generated by non-equilibrium thermodynamics.

ARXIV EPRINT: [1703.05162](https://arxiv.org/abs/1703.05162)

# 1 Introduction

In recent times, a lot of effort has been devoted to investigate the low-frequency, hydrodynamic limit of quantum field theories (QFTs) with holographic gravitational duals in the AdS/CFT framework. This hydrodynamic limit is a powerful tool to compute transport coefficients for strongly coupled QFTs, e.g. the quark-gluon plasma phase of QCD. In the hydrodynamic regime of thermal QFTs with gravitational duals, the shear viscosity to entropy density ratio  $\eta/s$  is of particular interest. In fact, this ratio takes the *universal* value  $1/4\pi$  for all QFTs with Einstein gravity duals [1–8]. This has led to conjecture the existence of a fundamental lower bound  $\eta/s \geq 1/4\pi$  — the Kovtun-Son-Starinets (KSS) bound [9] — which is supported both by energy-time uncertainty principle arguments and by quark-gluon plasma experimental data [9–11].

In the usual setting of the AdS/CFT correspondence, one utilises the holographic dualities to learn about transport coefficients in the hydrodynamic limit of strongly coupled QFTs by investigating bulk gravity configurations, typically black branes. However, this paradigm can be reversed and the properties of the dual QFT can be used to infer about the behaviour of bulk gravity solutions.<sup>1</sup> In this perspective, transport coefficients computed in the hydrodynamic limit of the dual QFT can lead to a deeper understanding of black hole (BH) physics. In particular, in this paper we aim to understand better the rich thermodynamical phase structure of AdS BHs with spherical horizons (characterised by meta-stabilities and Van der Walls-like behaviour [14–16]) by investigating the relationship between the shear viscosity of the dual QFT and the thermodynamics of these BHs.

By now, it is well-known that the KSS bound can be violated by two main different kinds of effects: higher-curvature terms in the Einstein-Hilbert action [17, 18] and breaking of the translational or rotational symmetry of the black brane background [19–27]. These two effects motivated us to consider spherical AdS BHs, for which the translational symmetry is intrinsically broken, both in general relativity (GR) and in a higher-curvature theory, namely Gauss-Bonnet (GB) gravity.

The violation of the KSS bound in higher-curvature gravity theories, although not completely understood, can be traced back to finite- $\mathcal{N}$ , finite- $\lambda_{tH}$  effects and to the inequality of the two central charges of the dual QFT [28, 29]. This lends support to the possibility of formulating modified bounds on  $\eta/s$ , based for instance on causality and positivity of energy in the dual QFT [30–32].

On the other hand, the violation of the KSS bound due to the breaking of translational symmetry has a more fundamental nature. In this case, the shear viscosity has not the usual hydrodynamic meaning but might be interpreted as the rate of entropy production due to a strain [20–24, 33]. In this framework, the behaviour of  $\eta/s$  as a function of the temperature  $T$  is non-trivial [34] and carries information about the infrared (IR) and ultraviolet (UV) behaviour of the QFT, the existence of global diffusive modes of the system and the nature of the effect responsible for the breaking of translational invariance. For instance, when this breaking is generated by the presence of a non-homogeneous scalar field in the bulk, the behaviour of  $\eta/s$  at small  $T$  is determined by the flow of the QFT in the IR. If the translational invariance is restored in the IR then  $\eta/s$  goes to a constant as  $T \rightarrow 0$ , signalling the presence of an IR collective diffusive mode. Conversely, if the translational invariance is not restored,  $\eta/s$  scales as  $T^{2\nu}$  for  $T \rightarrow 0$  and the IR geometry in  $D + 2$  dimensions is typically  $\text{AdS}_2 \times \mathbb{R}_D$  [23]. We will discuss the general validity of this behaviour for spherical BH backgrounds. In this case, the translational symmetry is intrinsically broken and cannot be restored in the IR, but holds only in the UV, where the spherical horizon can be approximated by a plane.

In a recent letter [35], we have proposed a definition of the shear viscosity for QFTs living in manifolds whose spatial sections are spheres. This has allowed us to compute the spherical

---

<sup>1</sup>For instance, this approach has been particularly fruitful for the computation of the microscopic entropy of BHs. In several cases, the Bekenstein-Hawking entropy has been matched by counting states in the dual CFT — see e.g. Refs. [12, 13].

analogue of the shear viscosity  $\tilde{\eta}$  for QFTs dual to five-dimensional AdS-Reissner-Nordström (AdS-RN) BHs in GR. Here, we present a detailed derivation of these results and extend the discussion to five-dimensional asymptotically AdS neutral and charged BHs in GB gravity.

We start by defining the (analogue) shear viscosity  $\tilde{\eta}$  for a QFT living on a  $D$ -sphere in the hydrodynamic limit. Although the shear viscosity has not the usual interpretation pertaining to a QFT in a translation-invariant background, we show that it still satisfies a Kubo formula and can be interpreted in terms of entropy production due to a strain. Then, following the approach of Refs. [23, 36], we compute  $\tilde{\eta}/s$  for QFTs dual to five-dimensional asymptotically AdS neutral and charged BHs in GR and GB gravity.

By considering linear perturbations of the field equations, the computation of  $\tilde{\eta}$  is reduced to the determination of the non-normalisable mode of the perturbation evaluated at the horizon. The perturbation satisfies a linear second-order differential equation analogous to a massive scalar equation in a curved background whose non-vanishing mass term encodes the breaking of translational invariance. Whereas the large and small  $T$  behaviours of  $\tilde{\eta}/s$  are determined analytically, its global behaviour is determined numerically. We show that for certain regimes of the temperature  $\tilde{\eta}/s$  is a monotonic function. It saturates the KSS bound at large  $T$  (or the GB coupling constant dependent bound in the GB case), where translational invariance is restored. When the BH has a regular, stable extremal limit  $\tilde{\eta}/s$  goes to zero with a  $T^{2\nu}$  scaling law at small temperatures.

An interesting and somehow unexpected behaviour of  $\tilde{\eta}/s$  emerges in the parameter regions where the BH has a Van der Walls-like behaviour (a second-order phase transition controlled by the charge or the GB coupling constant and a first-order phase transition — small/large BH — controlled by the temperature and characterised by a meta-stable intermediate region). In these regions, we find that  $\tilde{\eta}/s$  exhibits a temperature-dependent hysteresis and we explain this behaviour in terms of the non-equilibrium thermodynamics underlying the Van der Walls-like phase portrait.

The structure of the paper is as follows. In Sect. 2 we discuss the problems related with the hydrodynamic limit for QFTs dual to spherical BHs, the definition and the computation of  $\tilde{\eta}$  and we derive the Kubo formula for  $\tilde{\eta}$ . In Sect. 3 we review known facts about solutions, thermodynamics, phase structure and perturbations for AdS spherical BHs in GR and GB gravity. In Sect. 4 we give the general formula for  $\tilde{\eta}/s$ , compute its large and small  $T$  behaviours, give the numerical results for its global behaviour and discuss its relationship with the thermodynamical phase portrait of the dual BH solutions. Finally, in Sect. 5 we state our conclusions.

Throughout this paper indices  $a, b, \dots$  refer either to the whole  $D+2$ -dimensional bulk spacetime or also to its  $D+1$ -dimensional conformal boundary, while  $i, j, \dots$  refer to the transverse  $D$ -dimensional spatial sections.

## 2 Hydrodynamic limit for QFTs dual to spherical black holes and the analogue viscosity

Relativistic hydrodynamics is an effective long-distance description for a classical or quantum many-body system at non-zero temperature. In particular, it can be used to describe the non-equilibrium real-time macroscopic slow evolution of the system, both in space and time, with respect to a certain microscopic scale.

In the holographic framework of the AdS/CFT correspondence, the QFT lives in the boundary of a certain gravitational bulk region. In some cases, the QFT can be described by kinetic theory and the microscopic scale is determined by the mean free path of particles  $l_{\text{mfp}}$  and the typical momentum scale of the process  $k$ . When the kinetic theory is absent or unknown, it is still possible to give a thermal description and interpret the inverse temperature as the microscopic scale [37, 38]. Thus, the hydrodynamic limit of a QFT corresponds to large relaxation time, i.e. small frequencies,

and large scales compared to the typical one of the system, i.e.  $\tilde{\lambda} \gg 1/T \sim l_{\text{mfp}}$ , where  $\tilde{\lambda}$  is the wavelength of the excitations of the system.

In general, the existence of a hydrodynamic description is essentially due to the presence of conserved quantities, i.e. to the isometries of the system, whose densities can evolve (oscillate or relax to equilibrium) at arbitrarily long times provided the fluctuations are of large spatial size. Correspondingly, the expectation values of such densities are the hydrodynamic fields. However, it is still possible to give a hydrodynamic description of a system *without* conserved quantities in terms of expansion in derivatives of hydrodynamic fields (as the fluid velocity) [37]. We follow this approach to formulate the hydrodynamic description of a fluid in a spherical background holographically dual to AdS spherical BHs.

On the sphere, due to its intrinsic geometry, the translational invariance is broken. As a consequence, the momentum is not conserved and it is not possible to define an associated conserved current. At first sight, this should prevent us to study transport coefficients as the shear viscosity  $\eta$  which is, by definition, a measure of the momentum diffusivity due to a strain in a fluid. Hence, in principle, without translational symmetry it is not possible to define a conserved current, from which one can derive the Fick law of diffusion [39]. Nevertheless, as we will see below, we can circumvent these difficulties and give a rigorous definition of  $\eta$  for the hydrodynamic limit of a QFT in a spatial background without translational isometries.

Let us consider a QFT living on the boundary of  $\text{AdS}_{D+2}$  whose spatial sections have spherical topology. Although bulk BHs allow for dual QFTs living on a sphere [40–43], we are not interested in the explicit form of the holographically dual QFT. However, we can study its hydrodynamic limit in the sense described above. The boundary metric is conformal to  $\mathbb{R} \times S^D$

$$ds^2 = \frac{r^2}{L^2} (-dt^2 + L^2 d\bar{\Omega}_D^2), \quad (2.1)$$

where  $d\bar{\Omega}_D^2 = \bar{g}_{ij} dx^i dx^j$  is the metric of a  $D$ -sphere with constant curvature  $\kappa = 1$ . In this case, due to the spherical shape of the boundary, the metric perturbations used to describe the non-equilibrium real-time macroscopic slow evolution of the system are characterised by two parameters, the relaxation time or the frequency  $\omega$  and  $L/\ell$  which “measures” angular distances on the sphere. The integer number  $\ell$  parametrises the eigenvalue of the Lichnerowicz operator on the sphere (see eq. (2.8) below) and is analogous to the momentum scale  $k$  for a flat topology. In the spacetime (2.1), we define the hydrodynamic limit of the holographic QFT as the limit in which the metric perturbations have slow relaxation time and are much larger than the typical scale of the system, i.e.  $\omega \rightarrow 0$  and  $L/\ell \gg 1/T$ . Since we are dealing with a  $D$ -sphere, the number  $\ell$  cannot be arbitrarily small, i.e. there is a minimum value  $\ell_0$  [44–46] which corresponds to a maximum spatial scale, and to a maximum size for the global modes propagating on the sphere. On the contrary, in flat space, there is no constraint on the values of  $k$ , so one can set  $k \rightarrow 0$  which, in turns, corresponds to fluctuations of very large (in principle infinite) wavelength.

## 2.1 Hydrodynamics in curved spacetime

Relativistic hydrodynamics for a fluid in curved spacetimes can be formulated starting from the following definition for the stress-energy tensor [33, 37]

$$T^{ab} = \epsilon u^a u^b + T_{\perp}^{ab}, \quad (2.2)$$

where  $\epsilon$  is the energy density and the fluid velocity  $u^a$  (commonly evaluated in the frame in which the fluid is at rest) is timelike. The tensor  $T_{\perp}^{ab}$  is the spatial part of the stress-energy tensor and it is made by time-independent functions of the hydrodynamic variables  $\epsilon$ ,  $u^a$  and their derivatives. In a generic curved background, it is not always possible to define globally conserved currents associated

with symmetries of the system. However, we can always derive the hydrodynamic equations by requiring the stress-energy tensor to be covariantly conserved, i.e.  $\nabla_a T^{ab} = 0$ . In general, the hydrodynamic modes are infinitely slower than all other modes and the latter can be integrated out. Thus, all quantities appearing in the hydrodynamic equations are averaged over these fast modes and are functions of the slow-varying hydrodynamic variables.

Eq. (2.2) can be expanded in powers of derivatives of the velocity, and at first order, the most general expansion is given by

$$T^{ab} = (\epsilon + P) u^a u^b + P g^{ab} + \Pi^{ab}, \quad (2.3)$$

where  $P = P(\epsilon)$  is a scalar function and it can be interpreted as the thermodynamical pressure. The tensor  $\Pi^{ab}$  contains the derivatives of the fluid velocities, i.e. the dissipative contributions to  $T^{ab}$ . Its explicit form is given by [33, 37]<sup>2</sup>

$$\Pi^{ab} = -\eta \sigma^{ab} - \eta \tau_{\Pi} \left[ \langle \mathcal{D} \sigma^{ab} \rangle + \frac{1}{D} \sigma^{ab} (\nabla_c u^c) \right] + \left[ R^{(ab)} - (D-1) u_c R^{c(ab)d} u_d \right] + \dots \quad (2.4)$$

where the dots represent the non-linear terms in the fluid velocity, the parameter  $\eta = \eta(\epsilon)$  is the shear viscosity and  $\tau_{\Pi}$  is the relaxation time. The symbol  $\mathcal{D}$  represents the derivative with respect to the velocity direction, i.e.  $\mathcal{D} = u_a \nabla^a$ . The tensor  $\sigma^{ab}$  is a symmetric, transverse  $u_a \sigma^{ab} = 0$  and traceless  $g_{ab} \sigma^{ab} = 0$  tensor constructed with the first derivative in the fluid velocity given by  $\sigma^{ab} = 2 \langle \nabla^a u^b \rangle$ .

We conclude with some remarks about the conservation of the stress-energy tensor. For translation-invariant backgrounds, the conservation of the stress-energy tensor leads to the conservation of global currents and to the Fick law [39]. More generally, from the projection of  $\nabla_a T^{ab}$  along the fluid velocity  $u_b$ , one can relate second-order hydrodynamics with the second law of thermodynamics [37]. In particular, by using eqs. (2.3) and (2.4) one finds at linear order

$$\dot{s} = \frac{\eta}{2T} \sigma_{ij} \sigma^{ij}, \quad (2.5)$$

where  $s$  is the entropy density. Eq. (2.5) represents the rate of entropy production in a fluid due to a strain and it can be used to define the shear viscosity [23]. In our case, with the background metric (2.1) we can only consider local conservation since the translational invariance is broken and the Fick law is not satisfied but eq. (2.5) still holds.

## 2.2 Kubo formulas and the analogue viscosity

The Kubo formula relates thermal correlators to kinetic coefficients such as dissipative ones. For a relativistic QFT in flat spacetime, the Kubo formula gives a general definition of the shear viscosity in terms of the retarded Green function for the stress-energy tensor [10, 23, 47]

$$\eta = \lim_{\omega \rightarrow 0} \frac{1}{\omega} \text{Im} G_{T^{ij} T^{ij}}^R(\omega, k \rightarrow 0), \quad (2.6)$$

where  $i = x, j = y$ ,  $T^{ij}$  are the spatial components of the stress-energy tensor,  $\omega$  and  $k$  are the frequency and wave vector of the perturbation. When translational invariance is preserved and a hydrodynamic limit exists, eq. (2.6) becomes the Kubo formula for the transverse momentum. In this case,  $\eta$  defined by eq. (2.6) coincides with the usual hydrodynamical definition in terms of conserved quantities obtained from the Einstein relation  $C = \eta/sT$ , where  $C$  is the diffusion constant appearing in the Fick law [23]. In a holographic setup based on the AdS/CFT correspondence,

<sup>2</sup>For a rank-2 tensor,  $\langle A^{ab} \rangle = A^{(ab)} \equiv \frac{1}{2} \Delta^{ca} \Delta^{db} (A_{ab} + A_{ba}) - \frac{1}{D} \Delta^{ab} \Delta^{cd} A_{cd}$ , where  $\Delta^{ab}$  is a symmetric and transverse tensor given by  $\Delta^{ab} = g^{ab} + u^a u^b$ . In the local rest frame, it is the projector tensor on the spatial subspace.

$G_{T^{ij}T^{ij}}$  can be calculated using the usual AdS/CFT rules by considering small perturbations of the bulk metric.

In order to extend the Kubo formula (2.6) to spherical backgrounds, we consider small metric perturbations around the boundary background metric (2.1), i.e.  $g_{ab} \rightarrow g_{ab} + h_{ab}$ . Without loss of generality we choose transverse and traceless perturbations with  $h_{ab} = 0$  if  $(a, b) \neq (i, j)$ ,  $h_{ij} = h_{ij}(t, \mathbf{x})$ , where  $\mathbf{x}$  denote the angular directions. By inserting this type of perturbations in eq. (2.3) and considering the fluid at rest, i.e.  $u^a = (1, \mathbf{0})$ , we obtain

$$T^{ij} = -Ph_{ij} - \eta \dot{h}_{ij} + \eta \tau_{\Pi} \ddot{h}_{ij} - \frac{1}{2} \left[ (D-2) \ddot{h}_{ij} + L^2 \bar{\Delta}_L h_{ij} \right], \quad (2.7)$$

where  $\bar{\Delta}_L = \bar{\nabla}_k \bar{\nabla}^k$  is the Lichnerowicz operator and it corresponds to a generalisation of the Laplacian for the  $D$ -sphere, with  $D \geq 3$ . Eq. (2.7) is analogous to the one obtained in Ref. [37] for planar topology. As requested by linear response theory, we compute the retarded Green function for the tensor channel: by choosing a harmonic time dependence for the perturbation,  $h_{ij}(t, \mathbf{x}) = e^{-i\omega t} h_{ij}(\mathbf{x})$  and by expanding in hyper-spherical harmonics [48–50], we can extract the retarded Green function from eq. (2.7),

$$G_{T^{ij}T^{ij}}^R(\omega, \ell) = -P - i\omega\eta - \omega^2\eta\tau_{\Pi} - \frac{1}{2} \left[ (D-2)\omega^2 + L^2\gamma \right], \quad (2.8)$$

where  $\gamma = \ell(\ell + D - 1) - 2$  are the eigenvalues of the Lichnerowicz operator and  $\ell = 1, 2, 3, \dots$  is an integer associated with the hyper-spherical harmonic expansion. The eigenvalues  $\gamma$  are positive and form a discrete set [44–46, 50]. Given the retarded Green function above we can extract the dissipative coefficients  $\eta$  and  $\tau_{\Pi}$ . In particular, we are lead to define the analogue of shear viscosity in the hydrodynamic limit for a QFT in a spatial spherical background as,

$$\tilde{\eta} \equiv - \lim_{\omega \rightarrow 0} \frac{1}{\omega} \text{Im} G_{T^{ij}T^{ij}}^R(\omega, \ell \rightarrow \ell_0), \quad (2.9)$$

where  $\ell_0$  is the minimum value of  $\ell$ . Notice that the shear viscosity  $\tilde{\eta}$  in eq. (2.9) is defined as the  $\ell \rightarrow \ell_0$  limit of the retarded Green function in analogy with eq. (2.6). In planar hydrodynamics, the  $k \rightarrow 0$  limit describes long wavelength modes and probes large scales on the plane. In the spherical case, the  $\ell \rightarrow \ell_0$  modes probe large angles on the sphere.

It is also important to stress that, with respect to the planar case, the expression in square brackets in eq. (2.7) has an additional contribution to the stress-energy tensor ruled by the curvature. This is rather expected in view of the breaking of translational invariance. However, this additional contribution does not contribute to the shear viscosity.

### 3 Black hole solutions in five dimensions

The field equations of five-dimensional Einstein-Gauss-Bonnet gravity sourced by any form of matter fields described by the stress-energy tensor  $T_{(M)a}^b$  are [51–53]

$$G_{(1)a}^b + \alpha_2 G_{(2)a}^b = 8\pi G_5 T_{(M)a}^b, \quad (3.1)$$

where  $G_{(1)a}^b \equiv R_a^b - \frac{1}{2} R \delta_a^b$  is the Einstein tensor,  $\alpha_2$  is the GB coupling constant,  $G_5$  is the five-dimensional Newton constant, and  $G_{(2)a}^b$  is the GB contribution,

$$G_{(2)a}^b \equiv R_{ca}^{de} R_{de}^{cb} - 2R_d^c R_{ca}^{db} - 2R_a^c R_c^b + R R_a^b - \frac{1}{4} \delta_a^b (R_{cd}^{ef} R_{ef}^{cd} - 4R_c^d R_d^c + R^2). \quad (3.2)$$

For later convenience we define  $\lambda \equiv \alpha_2/L^2$ , being  $L$  the AdS length. Throughout this paper, the source term contains only a negative cosmological constant and an electromagnetic field. In

particular, we consider static  $\kappa = 1$  BH solutions to (3.1) in the form

$$ds^2 = -f(r) dt^2 + \frac{dr^2}{f(r)} + r^2 d\bar{\Omega}_3^2. \quad (3.3)$$

For the AdS-RN BHs of GR the metric function is

$$f_{\text{RN}}(r) = 1 + \frac{r^2}{L^2} - \frac{8G_5 M}{3\pi r^2} + \frac{4\pi G_5 Q^2}{3r^4}, \quad (3.4)$$

while, in the branch that allows for BH solutions, the metric function for GB gravity is

$$f_{\text{GB}}(r) = 1 + \frac{r^2}{2\lambda L^2} \left[ 1 - \sqrt{1 - 4\lambda L^2 \left( \frac{1}{L^2} - \frac{8G_5 M}{3\pi r^4} + \frac{4\pi G_5 Q^2}{3r^6} \right)} \right]. \quad (3.5)$$

In eqs. (3.4) and (3.5),  $M$  and  $Q$  are, respectively, the BH mass and charge.

### 3.1 Black holes in Gauss-Bonnet gravity

As in the black brane case, asymptotically AdS BH solutions of GB gravity exist only for  $\lambda < 1/4$ . Moreover, it is known that the unitarity bounds for the dual QFT constrain the value of  $\lambda$  [17, 54, 55], so that in this paper we will take  $\lambda$  in the following range  $0 < \lambda \leq 9/100$ .

The BH horizons are determined by the positive zeroes of the function

$$h(Y) = \frac{Y^3}{L^2} + Y^2 - \sigma Y + \rho, \quad (3.6)$$

where  $Y = r^2$ ,  $\sigma = 8G_5 M/3\pi - \lambda L^2$ ,  $\rho = 4\pi G_5 Q^2/3$ . The BH becomes extremal when  $h'(Y) = 0$ .

Asymptotically AdS BH solutions with inner ( $r_-$ ) and outer ( $r_+$ ) horizons exist for

$$M \geq \frac{3\pi}{8G_5} \left[ \lambda L^2 + \frac{L^2}{3} (z_0^2 + 2z_0) \right], \quad (3.7)$$

where  $z_0$  is the real, positive solution of the cubic equation  $2z^3 + 3z^2 - 27\rho/L^4 = 0$ . When the inequality is saturated, the inner and outer horizons merge, i.e. the BH becomes extremal and in the near-horizon regime the solution factorises as  $\text{AdS}_2 \times S^3$

$$ds^2 = -\frac{r^2}{l^2} dt^2 + \frac{l^2 dr^2}{r^2} + r_0^2 d\bar{\Omega}_3^2, \quad (3.8)$$

where  $r_0$  is BH radius at extremality, determined by the solution  $Y_0 = r_0^2$  of the cubic equation

$$h_{\text{ext}}(Y) = \frac{2Y^3}{L^2} + Y^2 - \rho = 0, \quad (3.9)$$

and  $l$  is the  $\text{AdS}_2$  length

$$l^{-2} = \frac{2h''(r_0)}{r_0^2 + 2\lambda L^2} = \frac{2(6r_0^2 + 2L^2)}{L^2(r_0^2 + 2\lambda L^2)}. \quad (3.10)$$

The BH thermodynamical parameters temperature  $T$ , mass  $M$  and entropy  $S$  can be expressed in terms of the horizon radius  $r_+$  as [53]

$$T(r_+) = \frac{1}{4\pi r_+(r_+^2 + 2\lambda L^2)} \left( \frac{4r_+^4}{L^2} + 2r_+^2 - \frac{8\pi G_5 Q^2}{3r_+^2} \right), \quad (3.11)$$

$$M(r_+) = \frac{3\pi r_+^4}{8G_5} \left( \frac{1}{L^2} + \frac{1}{r_+^2} + \frac{\lambda L^2}{r_+^4} + \frac{4\pi G_5 Q^2}{3r_+^6} \right), \quad (3.12)$$

$$S(r_+) = \frac{\pi^2 r_+^3}{2G_5} \left( 1 + \frac{6\lambda L^2}{r_+^2} \right). \quad (3.13)$$



The spherical geometry of the horizon introduces another scale in the system, i.e. the radius of the sphere, which couples in a non-trivial way to the higher-curvature terms in the equations of motion (3.1). This scale introduces a dependence on the GB coupling in the mass bound (3.7) and in the thermodynamical expression (3.11) to (3.13). As a result, the thermodynamical and near-horizon behaviours of the GB BHs are completely different from their brane counterparts. Indeed, for charged GB black branes, such behaviours are universal, i.e. do not depend on  $\lambda$ , and are essentially the same of the RN black branes of GR [26].

Notice that although the extremal radius  $r_0$  is determined only by the BH charge and the cosmological constant, the  $\text{AdS}_2$  length  $l$  and hence the extremal geometry (3.8) depend on the GB coupling constant. Notice also that the expression in the parenthesis in eq. (3.11) is proportional to  $h_{\text{ext}}(Y_+)$  meaning that the extremal geometry is obtained at zero temperature.

The thermodynamical parameters (3.11) to (3.13) near-extremality are

$$T(r_+) = \frac{2}{\pi L^2} \frac{3r_0^2 + L^2}{r_0^2 + 2\lambda L^2} (r_+ - r_0) + \mathcal{O}\left((r_+ - r_0)^2\right), \quad (3.14)$$

$$M(T) = \frac{3\pi}{8G_5} \left( \frac{3r_0^4}{L^2} + 2r_0^2 + \lambda L^2 \right) + \frac{3\pi^3}{8G_5} \frac{L^2(r_0^2 + 2\lambda L^2)^2}{L^2 + 3r_0^2} T^2 + \mathcal{O}(T^3), \quad (3.15)$$

$$S(T) = \frac{\pi^2 r_0^3}{2G_5} \left( 1 + \frac{6\lambda L^2}{r_0^2} \right) + \frac{3\pi^3}{4G_5} \frac{L^2(r_0^2 + 2\lambda L^2)^2}{L^2 + 3r_0^2} T + \mathcal{O}(T^2). \quad (3.16)$$

The first terms in the expressions (3.15) and (3.16) represent, respectively, the BH mass and entropy at extremality.

### 3.2 Phase structure of AdS-Reissner-Nordström black holes

Although the metric function  $f_{\text{GB}}$  in eq. (3.5) is singular for  $\lambda = 0$ , the thermodynamical behaviour of the charged AdS-RN solution can be simply obtained by putting  $\lambda = 0$  in eqs. (3.7) and (3.11) to (3.13).

To characterise the phase structure of these BHs, one can distinguish between two cases: fixed electric potential or fixed electric charge [14, 15]. In this paper we choose to fix the charge. As the charge of BH decreases to a critical value  $Q_c$ , the system undergoes a second-order phase transition. Below the critical charge, there are three possible branches of solutions that depend on the radius and therefore on the temperature of the system. For small temperatures, a small BH is the only locally stable solution; as the temperature increases, we have a meta-stable configuration describing intermediate BHs; for sufficiently high temperatures, large BHs are globally preferred. The evolution from small to large BHs through the meta-stable region corresponds to a first-order phase transition. Above the critical charge, the BH solution is always globally preferred. This behaviour can be understood by analysing the temperature as a function of the BH radius given by eq. (3.11) with  $\lambda = 0$ . For  $Q > Q_c$  it is a monotonic function, whereas it develops local extrema for  $Q < Q_c$  and an inflection point for  $Q = Q_c$ . The phase portrait of the AdS-RN BHs is very similar to a liquid/gas Van der Waals phase transition where the BH temperature plays the role of the pressure, the BH radius that of the volume and the BH charge that of the temperature [14, 15]. This portrait has been extended by Kubizňák *et al.* in Refs. [56, 57] and to topological AdS BHs in massive gravity [58].

### 3.3 Phase structure of neutral Gauss-Bonnet black holes

Neutral GB BH solutions and their thermodynamical parameters are obtained by putting  $Q = 0$  in eqs. (3.5) and (3.11) to (3.13). These BHs are characterised by the absence of a regular, zero temperature extremal limit which, in turns, means the absence of an IR fixed point for the dual QFT in the holographic description. For positive  $\lambda$ , the  $T = 0$  extremal limit is a state with  $r_+ = 0$ ,



zero entropy and positive non-vanishing mass. Therefore, the small temperature thermodynamical behaviour is always singular.

Neutral GB BHs exhibit an interesting phase structure. Differently from Einstein gravity, where small BHs are not stable and a thermal AdS state is energetically preferred [59, 60], in GB gravity there exists a stable small BH.<sup>3</sup> It starts with a small positive free energy, becomes unstable and evolves to a thermal AdS phase. Additionally, we also have the usual stable BH phase for large radii [42]. By inspecting the behaviour of the specific heat and the free energy, one finds that the phase structure of neutral GB BHs strictly depends on the values of the GB coupling constant and the BH radius [52]. For values of the GB coupling constant below the critical one,  $\lambda_c = 1/36$ , there are three different branches of solutions that correspond to small, intermediate and large BHs. The specific heat is positive in the first and third branch, whereas it is negative in the second branch. This behaviour is a consequence of the fact that  $T(r_+)$  given by eq. (3.11) with  $Q = 0$  is monotonically increasing for  $\lambda > \lambda_c$ , whereas it develops local extrema for  $\lambda < \lambda_c$  [52]. For  $\lambda \geq \lambda_c$  the second branch disappears and BHs are always locally stable but not necessarily globally preferred. Computing the free energy one finds that the BH solution is globally stable and energetically preferred with respect to thermal AdS in the parameter region  $\lambda_1(r_+) \leq \lambda \leq \lambda_2(r_+)$ , where  $\lambda_1(r_+)$  and  $\lambda_2(r_+)$  are some functions of the horizon radius [52]. Outside this region we have an Hawking-Page phase transition, BHs become globally unstable and thermal AdS is energetically preferred. Therefore, in the parameter region where BHs are energetically preferred with respect to thermal AdS, the phase diagram of uncharged GB BH has the same Van der Waals form described in the previous section for the AdS-RN BH, with the GB parameter  $\lambda$  playing the role of the BH charge  $Q$ .

### 3.4 Phase structure of charged Gauss-Bonnet black holes

The thermodynamical description of charged GB BHs is determined by the GB coupling constant  $\lambda$  and the charge  $Q$ . There are critical values of these parameters such that these BHs can exhibit the typical Van der Waals gas behaviour in the  $T$ - $S$  plane [62, 63].<sup>4</sup> Thus, charged GB BHs possesses both the Hawking-Page phase transition [16, 59] and a second-order one [63]. The former represents the transition from a stable AdS thermal state to a stable BH spacetime. Let  $T_c$  be the  $r_+$ -dependent critical value of the temperature and  $r_c^2 = 6\lambda L^2$ . Then, for  $T > T_c$  and  $r_+ > r_c$  (or  $T < T_c$  and  $r_+ < r_c$ ) AdS is preferred with respect to the BH, whereas for  $T < T_c$  and  $r_+ > r_c$  (or  $T > T_c$  and  $r_+ < r_c$ ), the BH is preferred with respect to AdS. It is remarkable that due to presence of  $\lambda$  and  $Q$ , the standard critical point becomes a critical line in the  $T$ - $r_+$  phase diagram [16].

Again, the phase portrait has the Van der Waals-like form described in Sects. 3.2 and 3.3 if one considers only the parameter region where the BH phase is globally preferred with respect to the thermal AdS phase and if one holds either  $Q$  or  $\lambda$  fixed. In the former (latter) case, at the critical value  $\lambda_c$  ( $Q_c$ ) the system undergoes a second-order phase transition. For  $\lambda < \lambda_c$  ( $Q < Q_c$ ), varying the temperature we have again a stable small BH phase and a stable large BH phase connected by a meta-stable phase. Moreover, the function  $T(r_+)$  has always the typical behaviour described in Sects. 3.2 and 3.3.

### 3.5 Linear perturbations in Einstein-Gauss-Bonnet gravity

In this section, we study linear tensorial perturbations about the background (3.3) in Einstein-Gauss-Bonnet gravity, i.e.  $g_{ab} \rightarrow g_{ab} + h_{ab}$ . After suitable manipulations, the linearised equation of

<sup>3</sup>Small BHs can be gravitationally unstable for values of  $\lambda$  larger than those considered here [61].

<sup>4</sup>This is analogous to consider the cosmological constant as a pressure term in the BH equation of state [64].

motion (3.1) are

$$\delta R_i^j + \lambda L^2 \delta G_{(2)i}^j + 8\pi G_5 \left( T_{(M)i}^k h_k^j - \frac{\delta T_{(M)ij}}{h_{ij}} h_i^j \right) = 0, \quad (3.17)$$

where  $\delta T_{(M)ij} = \left( \frac{\delta T_{(M)ij}}{h_{ij}} \right) h_{ij}$  and the explicit form of the tensors  $\delta R_i^j$  and  $\delta G_{(2)i}^j$  can be found in Refs. [65, 66]. In the transverse and traceless gauge ( $\nabla^a h_{ab} = g^{ab} h_{ab} = 0$ ), with  $h_{ab} = 0$  unless  $(a, b) = (i, j)$  we can write

$$h_{ij}(r, t, \mathbf{x}) = r^2 \phi(r, t) \bar{h}_{ij}(\mathbf{x}), \quad (3.18)$$

where  $\mathbf{x}$  is the direction of the sphere along which the perturbation propagates and  $\bar{h}_{ij}$  is the eigentensor of the Lichnerowicz operator built on the background 3-sphere

$$(\bar{\Delta}_L + \gamma) \bar{h}_{ij} = 0, \quad \gamma = \ell(\ell + 2) - 2. \quad (3.19)$$

The perturbations  $h_{ij}$  are both gauge-invariant and decouple [44–46, 65, 66]. This decoupling is a consequence of the spherical symmetry of the background and occur for every value of  $\ell$  and not only in the hydrodynamic limit  $\ell = \ell_0$ . Furthermore, assuming a harmonic time-dependence of the perturbation,  $h_i^j = \phi(r, t) \bar{h}_i^j(\mathbf{x}) = \psi(r) e^{-i\omega t} \bar{h}_i^j(\mathbf{x})$ , the perturbation  $h_i^j$  factorises leading to a set of equations which depend only on  $t$  and  $r$  [65, 66]. Thus eq. (3.17) reduces to a massive scalar equation

$$\frac{1}{r^3} \frac{d}{dr} \left[ r^3 f(r) F(r) \frac{d\psi(r)}{dr} \right] + \omega^2 \frac{F(r)}{f(r)} \psi(r) - m^2(r) \psi(r) = 0, \quad (3.20)$$

where  $F(r) \equiv 1 - \lambda L^2 f'(r)/r$  and the mass term is

$$m^2(r) = \frac{2 - \gamma}{r^2} [1 - \lambda L^2 f''(r)] + T_{(M)i}^i - \frac{\delta T_{(M)ij}}{\delta g_{ij}}. \quad (3.21)$$

Notice that the mass term depends on the angular part of the perturbation through the eigenvalue  $\gamma$  of the Lichnerowicz operator (3.19) and on higher-curvature corrections through the GB constant  $\lambda$ . In the black brane case, if translational invariance is preserved, the mass term is identically zero [10]. We stress that, although eq. (3.20) holds for any  $\ell$ , since we are interested in computing the shear viscosity (2.9), in the following we will take  $\ell$  equal to its minimum value  $\ell_0 = 1$  implying  $\gamma = 1$ .

There are no general exact analytical solutions of eq. (3.20), but we can find analytical approximate solutions for  $r \rightarrow \infty$  and in the near-horizon limit. In the generic case, one can compute the solutions only numerically.

The asymptotic solutions of eq. (3.20) with  $\omega = 0$  are given in terms of the modified Bessel functions of first and second kind. For  $r \rightarrow \infty$ , the non-normalisable mode  $\psi_0$  and the normalisable mode  $\psi_1$  behave as

$$\psi_0 = 1 - \frac{\lambda L^2}{2(1 - \sqrt{1 - 4\lambda}) r^2} + \mathcal{O}(\log r/r^4), \quad \psi_1 = \frac{1}{r^4} + \mathcal{O}(1/r^6). \quad (3.22)$$

In eq. (3.22) we have chosen the integration constant such that the non-normalisable mode  $\psi_0$  goes to 1 as  $r \rightarrow \infty$ .

The near-horizon behaviour of  $\psi_0(r)$  is different for non-extremal and extremal BHs. In the case of non-extremal BHs at temperature  $T$  and extremal  $T = 0$  BHs we write the metric function, respectively

$$f(r) = 4\pi T (r - r_+) + \frac{f''(r_+)}{2} (r - r_+)^2 + \mathcal{O}((r - r_+)^3), \quad (3.23)$$

$$f(r) = \frac{(r - r_0)^2}{l^2} + \mathcal{O}((r - r_+)^3), \quad (3.24)$$

where the extremal BH radius  $r_0$  is defined in eq. (3.9) and the AdS<sub>2</sub> length  $l$  is given by eq. (3.10). In the non-extremal case, we write  $\psi_0(r)$  using a power-series expansion, and we solve eq. (3.20) order by order. At leading order we find:

$$\psi_0(r) = \psi_0(r_+) \left[ 1 + \frac{1 - \lambda L^2 f''(r_+)}{4\pi T r_+^2 - \lambda L^2 r_+ (4\pi T)^2} (r - r_+) \right] + \mathcal{O}\left((r - r_+)^2\right). \quad (3.25)$$

For the extremal case, the leading quadratic behaviour of  $f(r)$  implies  $\psi_0(r_+) = 0$ . The behaviour of  $\psi_0(r)$  in the near-horizon region is

$$\psi_0(r) = (r - r_0)^\nu, \quad \nu = \frac{1}{2} \left( -1 + \sqrt{1 + \frac{4l^2 - 8\lambda L^2}{r_0^2}} \right). \quad (3.26)$$

#### 4 The shear viscosity to entropy density ratio

In this section, following the method proposed in Refs. [23, 36], we compute the shear viscosity to entropy ratio for the QFTs dual to the BH solutions discussed in Sect. 3. For Einstein gravity coupled to matter,  $\tilde{\eta}/s$  of the dual QFT is determined by means of the retarded Green function in eq. (2.9) and it is given by the non-normalisable mode  $\psi_0$  of the perturbation evaluated at the horizon,

$$\frac{\tilde{\eta}}{s} = \frac{1}{4\pi} \psi_0(r_+)^2. \quad (4.1)$$

This method can be generalised to include higher-curvature contributions. The computation uses a Wronskian method to determine the relation between the normalisable mode  $\psi_1$  and the non-normalisable mode  $\psi_0$ . Since this relation does not depend on the mass term  $m^2(r)$  in eq. (3.20), the formula of Ref. [23] also holds for BHs in GB gravity:

$$\frac{\tilde{\eta}}{s} = \frac{1}{4\pi} \psi_0(r_+)^2 \left[ 1 - 4\lambda \left( 1 - \frac{2\pi G_5 Q^2 L^2}{3r_+^6} \right) \right] \left( 1 + \frac{6\lambda L^2}{r_+^2} \right)^{-1}, \quad (4.2)$$

where  $\psi_0(r)$  is the non-normalisable solution of eq. (3.20) with  $\omega = 0$ .

For background solutions which do not break translational invariance, e.g. branes, the mass term  $m^2(r)$  is identically zero and the zero-frequency solution is  $\psi_0(r) = 1$  everywhere [23, 26]. On the contrary, in BH backgrounds, the translational invariance is broken, the mass term  $m^2(r)$  is non-vanishing, the  $\omega = 0$  solution for  $\psi_0(r)$  is not constant and  $\psi_0(r_+)$  must be calculated by integrating eq. (3.20) with  $\omega = 0$ .

Large radius BHs  $r_+ \gg L$ , correspond to the large temperature regime  $T \gg 1/L$ . In this approximation we can invert  $T(r_+)$  in eq. (3.11) to get  $r_+(T) = \pi L^2 T + \mathcal{O}(1/T)$ . Then, using eqs. (3.22) and (4.2) we get

$$\frac{\tilde{\eta}}{s} = \frac{1 - 4\lambda}{4\pi} \left[ 1 - \frac{\lambda L^2 (7 - 6\sqrt{1 - 4\lambda})}{\pi^2 (1 - \sqrt{1 - 4\lambda}) L^4 T^2} + \mathcal{O}(1/T^4) \right]. \quad (4.3)$$

As expected, in the large  $T$  regime,  $\tilde{\eta}/s$  does not depend on the charge. For GR BHs, eq. (4.3) is a decreasing function of the temperature, thus the KSS bound is violated and the universal value  $1/4\pi$  is attained only for  $T \rightarrow \infty$ . For GB BHs, the behaviour is qualitatively similar but as  $T \rightarrow \infty$  the value of  $\tilde{\eta}/s$  tends to  $(1 - 4\lambda)/4\pi$ .

In the extremal case, the metric function and its first derivative vanish when evaluated on the horizon and following Ref. [23] the shear viscosity to entropy ratio is given by

$$\frac{\tilde{\eta}}{s} = \frac{1}{4\pi} \psi_0(r_+)^2 \left( 1 + \frac{6\lambda L^2}{r_0^2} \right)^{-1}. \quad (4.4)$$

Eq. (3.26) tells us that  $\psi_0(r_+) = 0$ , which substituted in eq. (4.4) means that  $\tilde{\eta}/s$  goes to zero in the  $T = 0$  extremal limit. The scaling at low temperatures of  $\tilde{\eta}/s$  follows from simple matching argument [23] between scaling of the Green function and the near-horizon scaling (3.26)

$$\frac{\tilde{\eta}}{s} \sim T^{2\nu}, \quad (4.5)$$

where  $\nu$  is given by (3.26). The scaling exponent satisfies  $\nu \leq 1$  for

$$\lambda \geq \frac{l^4}{L^2 r_0^2} + \frac{l^2}{2L^2}. \quad (4.6)$$

The global behaviour of  $\tilde{\eta}/s$  as a function of  $T$  is obtained by numerically integrating eq. (3.20) supplied with a power-series boundary condition for  $\psi_0(r)$ . In the following, we choose units  $G_5 = L = 1$ . For each value of the charge and the GB parameter, there exists a minimum mass (and hence a minimum radius) given by eq. (3.7). We then integrate eq. (3.20) outwards from the horizon to infinity. Next, we use a shooting method to determine  $\psi_0(r_+)$  by requiring that  $\psi_0(\infty) = 1$ . Finally, the temperature and  $\tilde{\eta}/s$  for each solution are computed with eqs. (3.11) and (4.2).

#### 4.1 AdS Reissner-Nordström black holes

The plots of  $\tilde{\eta}/s$  resulting from our numerical calculations for GR are shown in fig. 1 for electrically neutral (left panel) and charged (right panel) BHs. The KSS bound is always violated for small and intermediate values of temperature, whereas it is saturated from below for large temperatures.

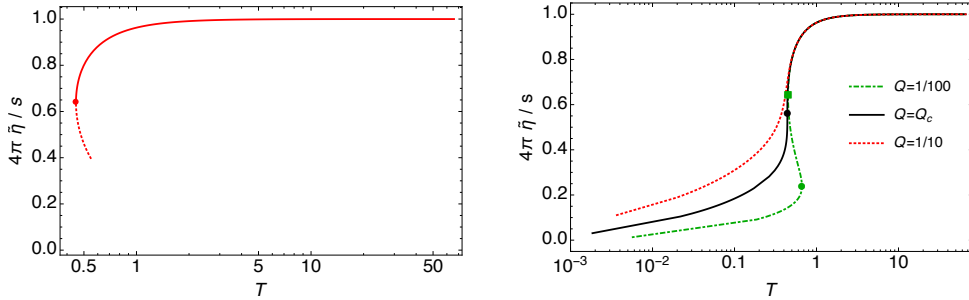


**Figure 1.** Global behaviour of  $\tilde{\eta}/s$  as a function of the temperature for GR BHs. *Left panel:* neutral AdS BHs. The solid line is the region above the critical radius, while the dotted line represents (part of) the region below the critical radius, where the BH is unstable and a thermal AdS solution is preferred; the dot marks the critical radius at  $T = \sqrt{2}/\pi$ . *Right panel:* AdS-RN BHs. We plot  $\tilde{\eta}/s$  for three selected values of the BH charge: above, at and below the critical value  $Q_c = 1/6\sqrt{5\pi}$ , at which the system undergoes the second-order phase transition. The dots (square) mark the maximum (minimum) of the temperature as a function of the BH radius.

In this section we extend the discussion of Ref. [35]. For neutral AdS BHs,  $\tilde{\eta}/s$  starts at the universal value  $1/4\pi$  at large temperatures and decreases monotonically as  $T$  decreases, reaching a minimum non-zero value for the non-vanishing minimum temperature  $T = \sqrt{2}/\pi$ . Such a temperature corresponds to the minimum value of the BH radius,  $r_0 = 1/\sqrt{2}$ . At  $r = r_0$  there is the Hawking-Page transition and for  $r_+ \leq r_0$  there are no stable BH solutions [60] and thermal AdS is energetically preferred with respect to the BH. The dotted line in the left panel of fig. 1 gives  $\tilde{\eta}/s$  for BHs with radii less than  $r_0$ , whose behaviour is a consequence of the growing of  $T$  for  $r_+ \leq r_0$ .

For AdS-RN BHs,  $\tilde{\eta}/s$  decreases from  $1/4\pi$  at large temperatures (independently from the charge), but the behaviour for small and intermediate temperatures depends on the charge. As explained in Sect. 3.2, there exists a critical value of the charge  $Q_c = 1/6\sqrt{5\pi}$  under which the

system undergoes a phase transition. On the right panel of fig. 1, we plot our numerical results for  $\tilde{\eta}/s$  for the critical charge and for representative values of the charge above, at and below the critical value. The dots (squares) in the curves with  $Q \leq Q_c$  mark the critical temperature  $T_{\max}$  ( $T_{\min}$ ) corresponding, to the two local extrema of the function  $T(r_+)$  of eq. (3.11). At these critical temperatures, the specific heat changes sign according to the discussion in Sect. 3.2. For  $Q = Q_c$  we have  $T_{\min} = T_{\max}$  and the function  $T(r_+)$  has an inflection point. For  $Q > Q_c$  the function  $T(r_+)$  is monotonically increasing and BHs are always stable. The numerical values  $T_{\min}$  and  $T_{\max}$  are listed in table 1 for a representative value of the charge below and at  $Q_c$ .

Interestingly,  $\tilde{\eta}/s$  develops hysteresis for  $Q < Q_c$ . This is evident for the  $Q = 1/100$  black solid curve in the right panel of fig. 1. We have also checked that curves with  $Q < Q_c$  have a similar hysteretic behaviour, whereas those with  $Q > Q_c$  (as the  $Q = 1/10$  orange dashed line) do not show this feature. This hysteretic behaviour is a direct consequence of the Van der Waals-like behaviour of the AdS-RN BHs discussed in Sect. 3.2. It is related to the presence of two local extrema in the function  $T(r_+)$  in eq. (3.11) or equivalently, to the presence of two stable states (small and large BHs) connected by a meta-stable region (intermediate BHs). This phase portrait has been considered as a general explanation of hysteretic behaviour for some variable of the system [67]. In particular, when the system evolves from high (low) to lower (higher) temperatures, a potential barrier prevents the evolution of the system from occurring as an equilibrium path between the two stable states [68]. Equilibrium will be reached passing through a meta-stable region and a path-dependence of  $\tilde{\eta}/s$  is generated. In particular, starting from high temperatures, the system will reach low temperatures going directly from the minimum and vice-versa. The presence of these local extrema determines the patterns of signs of the BH specific heat and free energy, hence the local thermodynamical stability [14, 52]. Thus, hysteresis in  $\tilde{\eta}/s$  and thermodynamical phase transition have the same origin and pattern. In fact, as already noted in Sect. 3.2, the phase diagram of AdS-RN BHs is very similar to that of a Van der Waals liquid/gas transition.

This is a very interesting result:  $\tilde{\eta}/s$  for the dual QFT carries direct information about the thermodynamic phase transitions of the system. In the holographic context, a hysteretic behaviour in the shear viscosity has been already observed in Ref. [19] for AdS BHs with broken rotational symmetry and with a p-wave holographic superfluid dual. Moreover, it is known that nanofluids may exhibit hysteresis in the  $\eta$ - $T$  plane [69].

Notice that, even though solutions with  $Q > Q_c$  describe stable BHs in the overall range of  $T$ , our numerical computation does not hold in the small  $T$  regime as it uses a power-series near-horizon expansion. However,  $\tilde{\eta}/s \rightarrow 0$  as  $T \rightarrow 0$  with analytical scaling law (4.5) and scaling exponent  $\nu$  given by eq. (3.26) with  $\lambda = 0$ .

## 4.2 Neutral Gauss-Bonnet black holes

Our numerical results for  $\tilde{\eta}/s$  as a function of  $T$  for neutral GB BHs are shown in fig. 2 for selected values of the GB parameter  $\lambda$  in the range  $0 < \lambda \leq 5/100$ .

For large temperatures, the KSS bound is always violated due to the GB contribution and  $4\pi\tilde{\eta}/s \rightarrow 1 - 4\lambda$ . At intermediate temperatures, the behaviour is qualitatively similar to that of RN BHs, with the GB parameter  $\lambda$  playing the role of the charge  $Q$ . As discussed in Sect. 3.3, there exists a critical value  $\lambda_c$  under which GB BHs can undergo a phase transition: by numerical investigation this value is  $\lambda_c = 1/36$ , in good agreement with Refs. [52, 63]. Curves with  $\lambda < \lambda_c$  (black solid and red dotted lines) show a hysteretic behaviour of  $\tilde{\eta}/s$  as a function of the temperature, whereas those with  $\lambda > \lambda_c$  do not. For a given value  $\lambda < \lambda_c$ , we have two critical temperatures  $T_{\max}, T_{\min}$ , which are marked respectively by dots and squares in the curves of fig. 2. Their numerical values for selected values of  $\lambda$  are listed in table 1. The physical interpretation of the appearance of hysteresis in  $\tilde{\eta}/s$  for the QFT dual to the neutral GB BH is completely analogue to that discussed

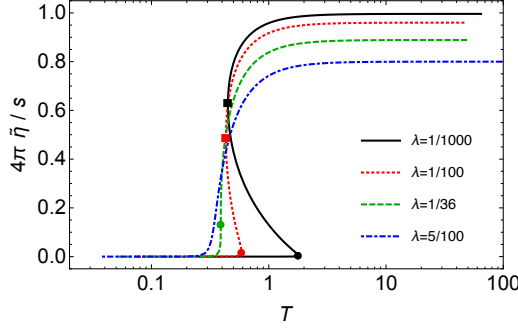


**Figure 2.** Global behaviour of  $\tilde{\eta}/s$  as a function of the temperature for GB BHs with  $Q = 0$  for selected values of the GB coupling constant above, at and below the critical value. Dots (squares) mark the maximum (minimum) of the temperature as a function of the BH radius.

for the AdS-RN BH. When  $\lambda$  reaches the critical value the system undergoes a second-order Van der Waals-like phase transition and exhibits the hysteretic behaviour in  $\tilde{\eta}/s$ .

### 4.3 Charged Gauss-Bonnet black holes

The presence of both a non-vanishing charge and GB coupling constant makes the case of charged GB BHs more involved. However, as discussed in Sect. 3.4, the phase portrait becomes much simpler and has a Van der Waals-like form if we restrict our considerations to the region where BHs are globally stable and holds either  $Q$  or  $\lambda$  fixed. In this situation we expect the qualitative behaviour of  $\tilde{\eta}/s$  as a function of  $T$  to be quite similar to that found for the AdS-RN and the neutral GB BHs.

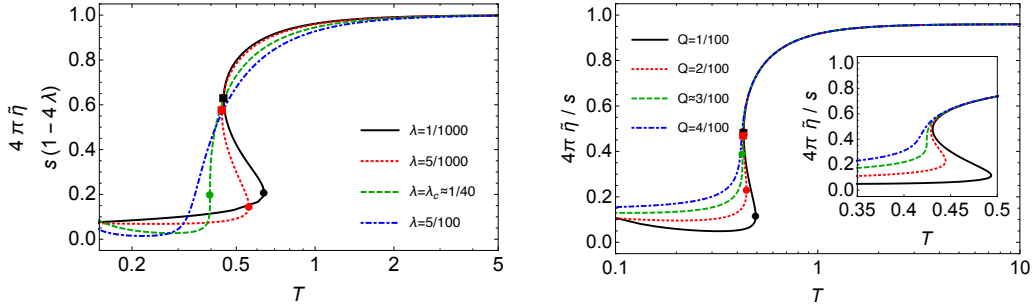


**Figure 3.** Global behaviour of  $\tilde{\eta}/s$  as a function of the temperature for charged GB BHs. *Left panel:* GB BHs with fixed charge  $Q = 1/100$ , and selected values of GB constant  $\lambda = 1/1000, 5/1000, \sim 0.25, 5/100$ . The value of  $\tilde{\eta}/s$  is rescaled by a factor  $1 - 4\lambda$ ; in this way the the large  $T$  behaviour of  $4\pi\tilde{\eta}/s$ , which for GB gravity is  $\lambda$ -dependent, has been normalised to 1. *Right panel:* GB BHs with fixed value of GB constant  $\lambda = 1/100$ , and selected values of charge  $Q = 1/100, 2/100, \sim 3/100, 4/100$ . Inset: zoom of the hysteresis region. Dots (squares) mark the local maximum  $T_{\max}$  (local minimum  $T_{\min}$ ) of the temperature.

The numerical results for  $\tilde{\eta}/s$  as a function of  $T$ , confirm our expectation and are shown in fig. 3 for  $Q$  fixed and selected values of the GB parameter  $\lambda$  (left panel) and for  $\lambda$  fixed and selected values of the charge  $Q$  (right panel). In both cases, the numerical results corroborate the analytical ones. For large temperatures, the KSS bound is always violated as  $4\pi\tilde{\eta}/s \rightarrow 1 - 4\lambda$ . At intermediate temperatures, the behaviour of  $\tilde{\eta}/s$  depends crucially on the values of the parameters  $Q$  and  $\lambda$ . For large values of  $Q$  (or for values of  $\lambda$  near to the unitarity bound  $\lambda \lesssim 9/100$ ), large BHs are always stable,  $\tilde{\eta}/s$  decreases monotonically with  $T$  and there is no hysteresis. The situation changes drastically for  $Q$  (or  $\lambda$ ) of order  $3/100$  and smaller: the system may undergo a Van der Waals-

like phase transition. The function  $T(r_+)$  develops two local extrema  $T_{\min}$  and  $T_{\max}$ , signalling the presence of two different stable thermodynamical phase (small and large BHs) connected by a meta-stable one, correspondingly, the  $\tilde{\eta}/s$  curve as a function of  $T$  develops hysteresis. Two typical examples of this hysteretic behaviour are shown in fig. 3. On the left panel, for fixed  $Q = 1/100$ , we see the onset of hysteresis, corresponding to the thermodynamical phase transition, when  $\lambda \lesssim 0.025$ . On the right panel, for fixed  $\lambda = 1/100$ , we see the onset of hysteresis and the thermodynamical phase transition when  $Q \lesssim 3/100$ . The corresponding values of the critical temperatures are marked by the dots ( $T_{\max}$ ) and squares ( $T_{\min}$ ) in fig. 3 and their numerical values are listed in table 1 for selected values of the parameters  $Q$  and  $\lambda$ . Analogous results can be found by choosing different  $Q$  and  $\lambda$ . Notice that, for stable BH solutions with values of  $\lambda$  and  $Q$  above the critical values, our numerical computation cannot reach  $T \sim 0$ , because it uses a power-series near-horizon expansion which does not hold in the extremal case. However, from eqs. (3.26) and (4.5), which describe analytically the near-extremal behaviour we conclude that  $\tilde{\eta}/s \rightarrow 0$  smoothly as  $T \rightarrow 0$ .

$Q$	1/100	$Q_c$	0			1/100			1/100	2/100	$Q_c$
$\lambda$	0	1/1000	1/100	$\lambda_c$	1/1000	5/1000	$\lambda_c$	1/100			
$T_{\min}$	0.449	0.441	0.448	0.431	0.390	0.448	0.440	0.397	0.431	0.429	0.425
$T_{\max}$	0.664	0.441	1.787	0.587	0.390	0.638	0.559	0.397	0.494	0.445	0.425

**Table 1.** Critical temperatures for selected values of  $\lambda$  and  $Q$  below and at the critical values. For the AdS-RN BH the critical charge is  $Q_c = 1/6\sqrt{5\pi}$ . For the neutral GB BH the critical value of the coupling is  $\lambda_c = 1/36$ . For GB BHs with fixed charge  $Q = 1/100$  the critical value of the coupling is  $\lambda_c \approx 1/4$ , while for fixed  $\lambda = 1/100$  the critical charge is  $Q_c \approx 3/100$ .

## 5 Summary and outlook

In this paper we have used the AdS/CFT correspondence to obtain information about the behaviour of bulk BHs by studying the hydrodynamic properties of the dual QFTs. In particular, we have defined and computed the shear viscosity to entropy ratio for QFTs holographically dual to five-dimensional AdS BH solutions of GR and GB gravity. In this way, we have extended the usual derivation of  $\tilde{\eta}/s$  for QFTs dual to gravitational bulk backgrounds with planar horizons to backgrounds with spherical horizons. We have shown that in holographic models the shear viscosity to entropy ratio of the QFT is closely related and keeps detailed information about the thermodynamical phase structure of the dual BH background. This is not completely unexpected, because experience with other holographic condensed matter system, like holographic superconductors, has shown us that transport features of the dual QFT may be strongly related to phase transitions of the dual black brane.

In general, the definition of a transport coefficient such as the shear viscosity is associated to the translational invariance of the system, i.e. the conservation of the momentum. As a consequence, from the associated conserved current one can derive the Fick law of diffusion. For systems that break translational invariance, the hydrodynamic interpretation in terms of conserved quantities fails but hydrodynamics can be still defined as an expansion in the derivatives of the hydrodynamic fields. In this way, it is possible to define the shear viscosity through a Kubo formula also for QFTs on a spherical background, see eq. (2.9), where the stress-energy tensor is only covariantly conserved. In addition, one can understand  $\tilde{\eta}$  as the rate of entropy production due to a strain, which is the typical interpretation when the homogeneity is broken by external matter fields. From this point of view, QFTs dual to spherical BHs are very similar to QFTs dual to black branes where the translational symmetry is broken by non-homogeneous external fields, e.g. scalars [23–25].



The definition of the hydrodynamic limit of a QFT on the sphere is plagued by an issue related to the compactness of the space. In fact, in a compact space, the usual hydrodynamic limit as an effective theory describing the long-wavelength modes of the QFT has not a straightforward interpretation. Our proposal is that for QFTs dual to bulk spherical BHs, the hydrodynamical, long wavelength modes can be described by the  $\ell \rightarrow \ell_0$  modes that probe large angles on the sphere. This is in analogy with the  $k \rightarrow 0$  modes for QFTs dual to bulk black branes which probe large scales on the plane. There is still a crucial difference between the two cases. When the breaking of translational symmetry is generated by external fields, the symmetry may be restored or not when the system flows to the IR [23]. In the BH case instead, because the breaking has a geometric and topological origin, translational symmetry cannot be restored in the IR.

As expected, the large  $T$  behaviour of  $\tilde{\eta}/s$ , corresponding to the flow to the UV fixed point, reproduces the universal value  $1/4\pi$  or  $(1 - 4\lambda)/4\pi$  in the GB case. When the bulk BH solution has a regular and stable extremal limit (like e.g. charged BHs) and remains stable at small  $T$ ,  $\tilde{\eta}/s \rightarrow 0$  as  $T \rightarrow 0$  with a  $T^{2\nu}$  scaling law. In this latter case, the system flows in the IR to the  $\text{AdS}_2 \times S^3$  geometry.

Our most important result is the behaviour of  $\tilde{\eta}/s$  at intermediate temperatures. A second-order Van der Waals-like phase transition occurs as the system goes from large values of  $Q$  and  $\lambda$  to the critical ones [14, 15]. Below the critical values of  $Q$  and  $\lambda$ , the BH undergoes a first-order phase transition controlled by the temperature. In this situation  $\tilde{\eta}/s$  as a function of  $T$  always develops hysteresis. The mechanism that generates hysteresis in  $\tilde{\eta}/s$  is the same that is responsible for the phase transition and can be traced back to non-equilibrium thermodynamics. When a control parameter, i.e. the charge  $Q$  or the GB coupling constant  $\lambda$ , is below its critical value, the function  $T(r_+)$  develops both a local maximum and minimum. The regions below the maximum and above the minimum correspond to two stable solutions, i.e. small and large BHs, respectively. The region between these two is represented by an unstable (meta-stable) region of intermediate BHs. When the system evolves from large (small) BHs to small (large) BHs, a potential barrier prevents the evolution of the system from occurring as an equilibrium path between the two stable states [68]. Equilibrium will be reached passing through a meta-stable region [67], and a path-dependence of  $\tilde{\eta}/s$  is generated. The presence of these local extrema determines the patterns of signs of the BH specific heat and free energy, hence the local thermodynamical stability [14, 52]. This interesting result represents the first attempt to infer about black hole thermodynamics through a detailed analysis of a transport coefficient as the shear viscosity.

## References

- [1] G. Policastro, D. T. Son, and A. O. Starinets, *The shear viscosity of strongly coupled  $N = 4$  supersymmetric Yang-Mills plasma*, *Phys. Rev. Lett.* **87** (2001) 081601, [[hep-th/0104066](#)].
- [2] A. Buchel, *On universality of stress-energy tensor correlation functions in supergravity*, *Phys. Lett.* **B609** (2005) 392, [[hep-th/0408095](#)].
- [3] P. Benincasa, A. Buchel, and R. Naryshkin, *The shear viscosity of gauge theory plasma with chemical potentials*, *Phys. Lett.* **B645** (2007) 309, [[hep-th/0610145](#)].
- [4] Y. Kats and P. Petrov, *Effect of curvature squared corrections in AdS on the viscosity of the dual gauge theory*, *JHEP* **01** (2009) 044, [[arXiv:0712.0743](#)].
- [5] K. Landsteiner and J. Mas, *The shear viscosity of the non-commutative plasma*, *JHEP* **07** (2007) 088, [[arXiv:0706.0411](#)].
- [6] N. Iqbal and H. Liu, *Universality of the hydrodynamic limit in AdS/CFT and the membrane paradigm*, *Phys. Rev.* **D79** (2009) 025023, [[arXiv:0809.3808](#)].

- [7] E. I. Buchbinder and A. Buchel, *The Fate of the Sound and Diffusion in Holographic Magnetic Field*, *Phys. Rev.* **D79** (2009) 046006, [[arXiv:0811.4325](#)].
- [8] M. Edalati, J. I. Jottar, and R. G. Leigh, *Transport Coefficients at Zero Temperature from Extremal Black Holes*, *JHEP* **01** (2010) 018, [[arXiv:0910.0645](#)].
- [9] P. Kovtun, D. T. Son, and A. O. Starinets, *Holography and hydrodynamics: Diffusion on stretched horizons*, *JHEP* **10** (2003) 064, [[hep-th/0309213](#)].
- [10] P. Kovtun, D. T. Son, and A. O. Starinets, *Viscosity in strongly interacting quantum field theories from black hole physics*, *Phys. Rev. Lett.* **94** (2005) 111601, [[hep-th/0405231](#)].
- [11] H. Song, S. A. Bass, U. Heinz, T. Hirano, and C. Shen, *200 A GeV Au+Au collisions serve a nearly perfect quark-gluon liquid*, *Phys. Rev. Lett.* **106** (2011) 192301, [[arXiv:1011.2783](#)]. [Erratum: *ibid.* **109** (2012) 139904].
- [12] A. Strominger and C. Vafa, *Microscopic origin of the Bekenstein-Hawking entropy*, *Phys. Lett.* **B379** (1996) 99, [[hep-th/9601029](#)].
- [13] M. Cadoni and S. Mignemi, *Entropy of 2-D black holes from counting microstates*, *Phys. Rev.* **D59** (1999) 081501, [[hep-th/9810251](#)].
- [14] A. Chamblin, R. Emparan, C. V. Johnson, and R. C. Myers, *Charged AdS black holes and catastrophic holography*, *Phys. Rev.* **D60** (1999) 064018, [[hep-th/9902170](#)].
- [15] A. Chamblin, R. Emparan, C. V. Johnson, and R. C. Myers, *Holography, thermodynamics and fluctuations of charged AdS black holes*, *Phys. Rev.* **D60** (1999) 104026, [[hep-th/9904197](#)].
- [16] M. Cvetič, S. Nojiri, and S. D. Odintsov, *Black hole thermodynamics and negative entropy in de Sitter and anti-de Sitter Einstein-Gauss-Bonnet gravity*, *Nucl. Phys.* **B628** (2002) 295, [[hep-th/0112045](#)].
- [17] M. Brigante, H. Liu, R. C. Myers, S. Shenker, and S. Yaida, *Viscosity Bound Violation in Higher Derivative Gravity*, *Phys. Rev.* **D77** (2008) 126006, [[arXiv:0712.0805](#)].
- [18] A. Bhattacharyya and D. Roychowdhury, *Viscosity bound for anisotropic superfluids in higher derivative gravity*, *JHEP* **03** (2015) 063, [[arXiv:1410.3222](#)].
- [19] J. Erdmenger, P. Kerner, and H. Zeller, *Non-universal shear viscosity from Einstein gravity*, *Phys. Lett.* **B699** (2011) 301, [[arXiv:1011.5912](#)].
- [20] A. Rebhan and D. Steineder, *Violation of the Holographic Viscosity Bound in a Strongly Coupled Anisotropic Plasma*, *Phys. Rev. Lett.* **108** (2012) 021601, [[arXiv:1110.6825](#)].
- [21] K. A. Mamo, *Holographic RG flow of the shear viscosity to entropy density ratio in strongly coupled anisotropic plasma*, *JHEP* **10** (2012) 070, [[arXiv:1205.1797](#)].
- [22] R. A. Davison, B. Goutéraux, and S. A. Hartnoll, *Incoherent transport in clean quantum critical metals*, *JHEP* **10** (2015) 112, [[arXiv:1507.07137](#)].
- [23] S. A. Hartnoll, D. M. Ramirez, and J. E. Santos, *Entropy production, viscosity bounds and bumpy black holes*, *JHEP* **03** (2016) 170, [[arXiv:1601.02757](#)].
- [24] P. Burikham and N. Poovuttikul, *Shear viscosity in holography and effective theory of transport without translational symmetry*, *Phys. Rev.* **D94** (2016) 106001, [[arXiv:1601.04624](#)].
- [25] L. Alberte, M. Baggioli, and O. Pujolas, *Viscosity bound violation in holographic solids and the viscoelastic response*, *JHEP* **07** (2016) 074, [[arXiv:1601.03384](#)].
- [26] M. Cadoni, A. M. Frassino, and M. Taveri, *On the universality of thermodynamics and  $\eta/s$  ratio for the charged Lovelock black branes*, *JHEP* **05** (2016) 101, [[arXiv:1602.05593](#)].
- [27] H.-S. Liu, H. Lu, and C. N. Pope, *Magnetically-Charged Black Branes and Viscosity/Entropy Ratios*, *JHEP* **12** (2016) 097, [[arXiv:1602.07712](#)].
- [28] A. Buchel, J. T. Liu, and A. O. Starinets, *Coupling constant dependence of the shear viscosity in  $N = 4$  supersymmetric Yang-Mills theory*, *Nucl. Phys.* **B707** (2005) 56, [[hep-th/0406264](#)].

- [29] A. Buchel, R. C. Myers, and A. Sinha, *Beyond  $\eta/s = 1/4\pi$* , *JHEP* **03** (2009) 084, [[arXiv:0812.2521](#)].
- [30] M. Brigante, H. Liu, R. C. Myers, S. Shenker, and S. Yaida, *The Viscosity Bound and Causality Violation*, *Phys. Rev. Lett.* **100** (2008) 191601, [[arXiv:0802.3318](#)].
- [31] A. Buchel and R. C. Myers, *Causality of Holographic Hydrodynamics*, *JHEP* **08** (2009) 016, [[arXiv:0906.2922](#)].
- [32] D. M. Hofman, *Higher Derivative Gravity, Causality and Positivity of Energy in a UV complete QFT*, *Nucl. Phys.* **B823** (2009) 174, [[arXiv:0907.1625](#)].
- [33] P. Romatschke, *Relativistic Viscous Fluid Dynamics and Non-Equilibrium Entropy*, *Class. Quantum Grav.* **27** (2010) 025006, [[arXiv:0906.4787](#)].
- [34] S. Cremonini, U. Gürsoy, and P. Szepietowski, *On the Temperature Dependence of the Shear Viscosity and Holography*, *JHEP* **08** (2012) 167, [[arXiv:1206.3581](#)].
- [35] M. Cadoni, E. Franzin, and M. Taveri, *Van der Waals-like Behaviour of Charged Black Holes and Hysteresis in the Dual QFTs*, *Phys. Lett. B* (2017) in press, [[arXiv:1702.08341](#)].
- [36] A. Lucas, *Conductivity of a strange metal: from holography to memory functions*, *JHEP* **03** (2015) 071, [[arXiv:1501.05656](#)].
- [37] R. Baier, P. Romatschke, D. T. Son, A. O. Starinets, and M. A. Stephanov, *Relativistic viscous hydrodynamics, conformal invariance, and holography*, *JHEP* **04** (2008) 100, [[arXiv:0712.2451](#)].
- [38] P. Kovtun, *Lectures on hydrodynamic fluctuations in relativistic theories*, *J. Phys.* **A45** (2012) 473001, [[arXiv:1205.5040](#)].
- [39] D. T. Son and A. O. Starinets, *Viscosity, Black Holes, and Quantum Field Theory*, *Ann. Rev. Nucl. Part. Sci.* **57** (2007) 95, [[arXiv:0704.0240](#)].
- [40] S. S. Gubser, I. R. Klebanov, and A. M. Polyakov, *Gauge theory correlators from noncritical string theory*, *Phys. Lett.* **B428** (1998) 105, [[hep-th/9802109](#)].
- [41] E. Witten, *Anti-de Sitter space and holography*, *Adv. Theor. Math. Phys.* **2** (1998) 253, [[hep-th/9802150](#)].
- [42] Y. M. Cho and I. P. Neupane, *Anti-de Sitter black holes, thermal phase transition and holography in higher curvature gravity*, *Phys. Rev.* **D66** (2002) 024044, [[hep-th/0202140](#)].
- [43] I. P. Neupane and N. Dadhich, *Entropy Bound and Causality Violation in Higher Curvature Gravity*, *Class. Quantum Grav.* **26** (2009) 015013, [[arXiv:0808.1919](#)].
- [44] H. Kodama and A. Ishibashi, *A master equation for gravitational perturbations of maximally symmetric black holes in higher dimensions*, *Prog. Theor. Phys.* **110** (2003) 701, [[hep-th/0305147](#)].
- [45] A. Ishibashi and H. Kodama, *Stability of higher dimensional Schwarzschild black holes*, *Prog. Theor. Phys.* **110** (2003) 901, [[hep-th/0305185](#)].
- [46] G. Gibbons and S. A. Hartnoll, *A gravitational instability in higher dimensions*, *Phys. Rev.* **D66** (2002) 064024, [[hep-th/0206202](#)].
- [47] G. Policastro, D. T. Son, and A. O. Starinets, *From AdS/CFT correspondence to hydrodynamics*, *JHEP* **09** (2002) 043, [[hep-th/0205052](#)].
- [48] M. A. Rubin and C. R. Ordóñez, *Eigenvalues and Degeneracies for n-dimensional tensor spherical harmonics*, *J. Math. Phys.* **25** (1984) 2888.
- [49] M. A. Rubin and C. R. Ordóñez, *Symmetric Tensor Eigen Spectrum of the Laplacian on n Spheres*, *J. Math. Phys.* **26** (1985) 65.
- [50] A. Higuchi, *Symmetric Tensor Spherical Harmonics on the N Sphere and Their Application to the de Sitter Group  $SO(N,1)$* , *J. Math. Phys.* **28** (1987) 1553. [Erratum: *ibid.* **43** (2002) 6385].

- [51] R. C. Myers and J. Z. Simon, *Black Hole Thermodynamics in Lovelock Gravity*, *Phys. Rev.* **D38** (1988) 2434.
- [52] R.-G. Cai, *Gauss-Bonnet black holes in AdS spaces*, *Phys. Rev.* **D65** (2002) 084014, [[hep-th/0109133](#)].
- [53] R.-G. Cai, *A note on thermodynamics of black holes in Lovelock gravity*, *Phys. Lett.* **B582** (2004) 237, [[hep-th/0311240](#)].
- [54] X.-H. Ge, Y. Matsuo, F.-W. Shu, S.-J. Sin, and T. Tsukioka, *Viscosity Bound, Causality Violation and Instability with Stringy Correction and Charge*, *JHEP* **10** (2008) 009, [[arXiv:0808.2354](#)].
- [55] X.-H. Ge and S.-J. Sin, *Shear viscosity, instability and the upper bound of the Gauss-Bonnet coupling constant*, *JHEP* **05** (2009) 051, [[arXiv:0903.2527](#)].
- [56] D. Kubizňák and R. B. Mann, *P-V criticality of charged AdS black holes*, *JHEP* **07** (2012) 033, [[arXiv:1205.0559](#)].
- [57] D. Kubizňák, R. B. Mann, and M. Teo, *Black hole chemistry: thermodynamics with Lambda*, *Class. Quantum Grav.* **34** (2017) 063001, [[arXiv:1608.06147](#)].
- [58] S. H. Hendi, R. B. Mann, S. Panahiyan, and B. Eslam Panah, *van der Waals like behavior of topological AdS black holes in massive gravity*, *Phys. Rev.* **D95** (2017) 021501, [[arXiv:1702.00432](#)].
- [59] S. W. Hawking and D. N. Page, *Thermodynamics of Black Holes in anti-De Sitter Space*, *Commun. Math. Phys.* **87** (1983) 577.
- [60] D. Birmingham, *Topological black holes in Anti-de Sitter space*, *Class. Quantum Grav.* **16** (1999) 1197, [[hep-th/9808032](#)].
- [61] R. A. Konoplya and A. Zhidenko, *Eikonal instability of Gauss-Bonnet-(anti-)de Sitter black holes*, [[arXiv:1701.01652](#)].
- [62] C. Hu, X. Zeng, and X. Liu, *Phase transition and critical phenomenon of AdS black holes in Einstein-Gauss-Bonnet gravity*, *Sci. China Phys. Mech. Astron.* **56** (2013) 1652.
- [63] S. He, L.-F. Li, and X.-X. Zeng, *Holographic Van der Waals-like phase transition in the Gauss-Bonnet gravity*, *Nucl. Phys.* **B915** (2017) 243, [[arXiv:1608.04208](#)].
- [64] A. M. Frassino, D. Kubizňák, R. B. Mann, and F. Simovic, *Multiple Reentrant Phase Transitions and Triple Points in Lovelock Thermodynamics*, *JHEP* **09** (2014) 080, [[arXiv:1406.7015](#)].
- [65] G. Dotti and R. J. Gleiser, *Gravitational instability of Einstein-Gauss-Bonnet black holes under tensor mode perturbations*, *Class. Quantum Grav.* **22** (2005) L1, [[gr-qc/0409005](#)].
- [66] G. Dotti and R. J. Gleiser, *Linear stability of Einstein-Gauss-Bonnet static spacetimes. Part I. Tensor perturbations*, *Phys. Rev.* **D72** (2005) 044018, [[gr-qc/0503117](#)].
- [67] D. R. Knittel, S. P. Pack, S. H. Lin, and L. Eyring, *A thermodynamic model of hysteresis in phase transitions and its application to rare earth oxide systems*, *J. Chem. Phys.* **67** (1977) 134.
- [68] G. Bertotti, *Hysteresis in Magnetism: For Physicists, Materials Scientists, and Engineers*. Academic Press, San Diego, CA, USA, 1998.
- [69] C. T. Nguyen, F. Desgranges, N. Galanis, G. Roy, T. Maré, S. Boucher, and H. Angue Mintsa, *Viscosity data for Al<sub>2</sub>O<sub>3</sub>-water nanofluid-hysteresis: is heat transfer enhancement using nanofluids reliable?*, *Int. J. Therm. Sci.* **47** (2008) 103.